MDPI

Article

Fencing Can Alter Gene Flow of Asian Elephant Populations within Protected Areas

Jean-Philippe Puyravaud [1], Samuel A. Cushman [2], P. Anuradha Reddy [3], Durairaj Boominathan [4], Reeta Sharma [5], Neelakantan Arumugam [6], Kanagaraj Muthamizh Selvan [7], Nagarathinam Mohanraj [4], Sedupathy Arulmozhi [8], Abdul Rahim [8], Tamanna Kalam [8], Rahul De [5], Swati Udayraj [8], Andrea Luis [8], Muneer Ul Islam Najar [8], Kothandapani Raman [9], Bawa Mothilal Krishnakumar [8], Surendra Prakash Goyal [5] and Priya Davidar [8,*]

1 Sigur Nature Trust, Mavinhalla PO, Nilgiris 643223, India
2 Rocky Mountain Research Station, Flagstaff, AZ 86001, USA
3 Centre for Cellular and Molecular Biology, Hyderabad 500030, India
4 WWF-India, Edayarpalayam, Coimbatore 641025, India
5 Wildlife Institute of India, Dehradun 248001, India
6 Department of Biotechnology, Pondicherry University, Puducherry 605014, India
7 Ministry of Environment, Forest & Climate Change, New Delhi 110003, India
8 Department Ecology and Environmental Sciences, Pondicherry University, Puducherry 605014, India
9 Indigenous Biodiversity Foundation, Pondicherry 605001, India
* Correspondence: pdavidar@gmail.com

Abstract: The Asian elephant is mostly confined to mountainous ranges and therefore risks population fragmentation if hard protected area (PA) boundaries near steep slopes prevent movement. We tested whether elephant gene flow is (i) controlled by slope and (ii) affected by the interplay between barriers and slope. We used 176 unique genotypes obtained non-invasively from fresh elephant dung to assess individual-by-individual genetic distance across the Western Ghats of India, a biodiversity hotspot. To assess landscape distance, 36 resistance models were produced by transforming a slope raster. Core areas and corridors were calculated from the raster that provided the best correlation between the genetic and distance matrices. The influence of the closure of PAs on gene flow was examined for one region, the Nilgiri Biosphere Reserve. The best resistance raster obtained by transforming the slope occupancy model was better than Euclidean distance for explaining genetic distance, indicating that slope partially controls gene flow. Fencing elephant PAs on hilly terrain reduces core areas and disrupts corridors. Consequently, hard PA boundaries abutting slopes can fragment elephant populations, but this can be ameliorated by protecting the adjacent flatter terrain.

Keywords: Asian elephant; slope; protected area; gene flow; connectivity

1. Introduction

The location and design of terrestrial protected areas (PAs) have been influenced by administrative convenience, economics, and human occupancy [1], with limited consideration for optimal conservation outcomes. Reserve boundaries often mark abrupt transitions between habitat and human-dominated areas because human population growth near PAs has been especially rapid in recent decades [2,3], driving the destruction of peripheral habitats [4]. In order to mitigate issues with problematic animals along hard boundaries between natural and human-dominated landscapes, reserve boundaries can be partially or totally closed with fences or trenches [5], for example in Sri Lanka [6], India [7], or Africa [8]. The question then arises whether enclosures alter gene flow within PAs.

The Asian elephant (*Elephas maximus*, called "the elephant" unless specified otherwise) was historically present across most of south and southeast Asia but is now largely confined to mountainous ranges [9]. Elephants avoid steep inclines [10] due to the energy required to transport their mass uphill [11] and probably also because of heat dissipation [12], relative

body strength [13], and risk perception [14]. Reserve boundaries that become impenetrable to elephant movement may combine with the effect of slope to fragment populations within PAs.

Landscape genetics can help to understand how geographical and environmental features structure genetic variation and gene flow [15]. Microsatellite data collected at multiple locations, from dung samples, for example, can be used to calculate genetic distance among individuals (see Peterson et al. [16] for a critical review). Genetic distance matrices among individuals can then be compared to landscape distance matrices among the same animals. Landscape distances are measured on resistance rasters provided by the transformations of variables hypothesized to be important for animal movement [17]. The transformations are essentially hypotheses regarding the functional effect the variables of interest have on the genetic distance among individuals. The best fit is obtained by comparing genetic and landscape distance matrices in a model selection framework. The raster providing the best fit is then selected to be a resistance layer in subsequent modeling to predict core areas and corridors [18].

In order to determine whether the closure of reserves reduces the gene flow of elephant populations within PAs, we focused on the Western Ghats of India (WG) (Figure 1), a biodiversity hotspot [19] where the elephant range spreads from 8°23′ N to around 16° N [9].
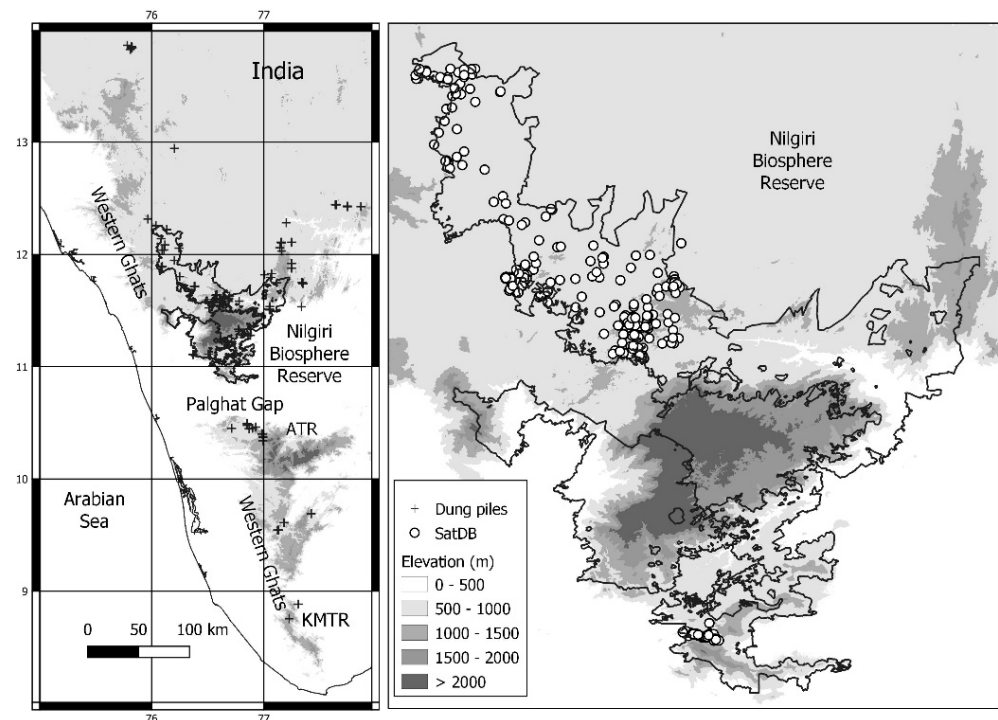

Figure 1. Study area: distribution of the dung samples over the Western Ghats and locations of the satellites fixed north (Nilgiri Biosphere Reserve) and south (Anamalai Tiger Reserve (ATR)—Kalakkad Mundanthurai Tiger Reserve (KMTR) of the Palghat Gap).

The WG is an escarpment running north–south along the western coastline of India, interrupted towards the south by the low-lying Palghat Gap that separates the northern from the southern elephant populations. This gap has been transformed by agriculture for several centuries, is 3 km at its narrowest, and 40 km at its widest. The northern part of the WG includes the Nilgiri Biosphere Reserve (NBR) and its surrounding PAs, which contain the largest remaining population of wild elephants, ca. 6000 animals [20]. The large number of recorded incidents with elephants at some sites [21] could potentially lead to the closure of PAs.

We used genetic data obtained over most of the WG for the landscape genetic analysis (Figure 1). A recent paper [22] across the elephant ranges in India found a partial genetic

differentiation between the northern and southern WG populations. Our objective was to focus on the genetic distance among individuals, not to study the elephant population genetics structure per se, which has already been covered in detail by De et al. [22]. We verified whether genetic differentiation between the northern and the southern parts of the WG affected the selection of the best connectivity model.

We calculated pairwise, individual-by-individual genetic distances for 176 elephant genotypes generated with seven microsatellite markers. We transformed a slope raster over the WG to select various resistance hypotheses (Figure 2). From these resistance maps, 35 landscape distance matrices among the 176 genotyped elephants were obtained, to which a Euclidean distance matrix was added. Correlations between genetic distance and landscape distance matrices were assessed by linear mixed-effect models [20].
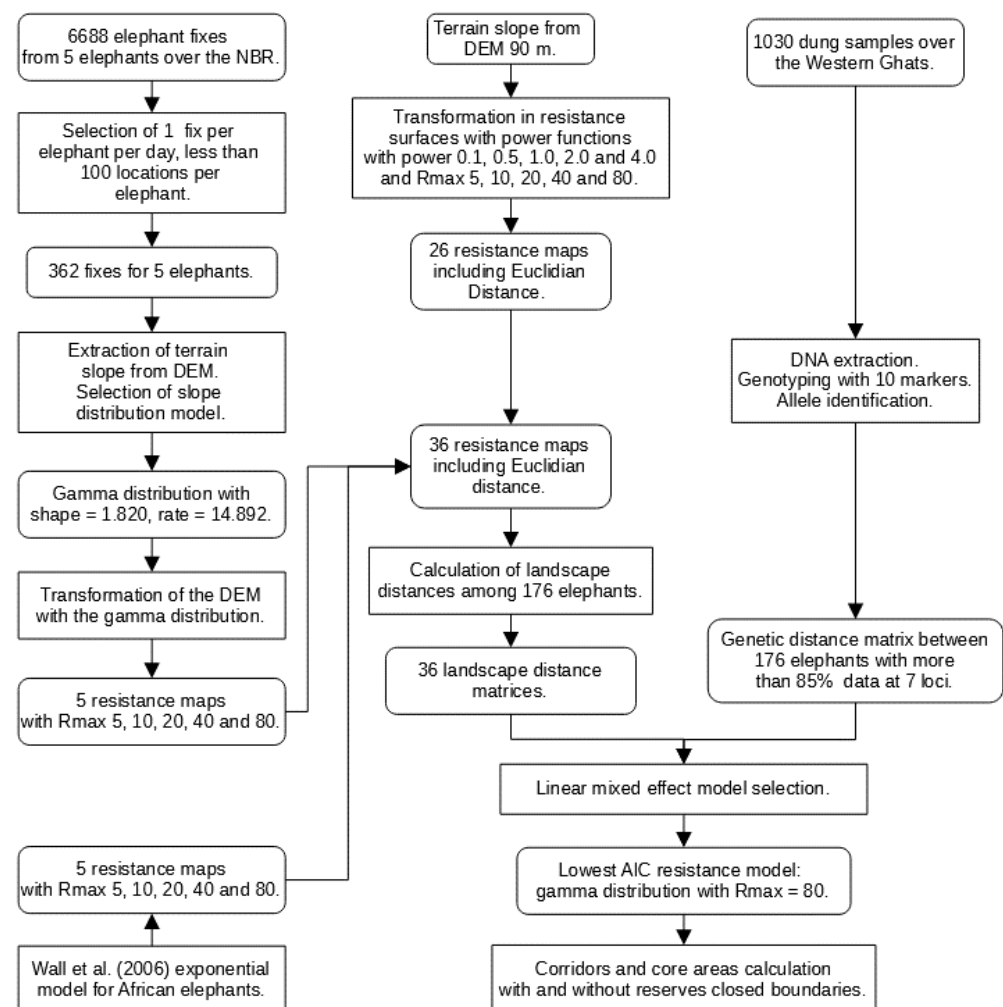
Figure 2. Method flowchart with the main components: (i) production of 36 resistance maps, (ii) calculation of landscape distance matrices, (iii) calculation of the genetic distance matrix, and (iv) calculation of core areas and corridors [11].

Genetic connectivity relative to slope was described by modeling core areas and corridors from the best resistance raster over the NBR. The NBR provides an adequate scale for examining the shrinkage of core areas and the disruption of corridors with fencing. For both core areas and corridor maps, we assumed two opposite and extreme situations. The first set of simulations considered the NBR boundary to be entirely porous, and the second considered it completely closed. These conditions are extreme, as in reality, most reserves have locations with porous boundaries and others with closed boundaries. The

two scenarios—entirely open or entirely closed PAs—can nevertheless address the question of whether enclosure affects the connectivity adjacent to the PA boundary.

We tested the null hypotheses that (i) elephant gene flow is associated with Euclidean distance instead of terrain slope and (ii) that gene flow within the NBR was not affected by the interplay between the closure of its boundaries and slopes.

2. Materials and Methods

2.1. Study Area and Sample Collection

The sampling was carried out at the administrative subdivision level (called "range") in each PA to maximize the coverage of elephant distribution (Figure 1). The northern elephant population in the NBR (which includes the Nilgiri–Brahmagiri–Eastern Ghats range) numbers around 6000 and the southern range (including the Anamalais–Nelliampathy–High Range and Megamalai–Periyar–Agastyamalai), here termed ATR-KMTR (Anamalai Tiger Reserve and Kalakad Mundanthurai Tiger Reserve), harbors around 4500 elephants [20]. Fresh elephant dung samples were collected between 2014 and 2018 from 1030 locations. The geographic coordinates were noted, and the surface layer of the dung was scraped into 50 mL Tarson tubes with absolute ethanol. Samples were stored at −20 °C after transportation to the laboratory.

2.2. DNA Extraction and Analysis

DNA extraction and analysis follow Parida et al. [23]. DNA was extracted using a QIAamp DNA stool kit (Qiagen, Hilden, Germany). We originally used ten polymorphic di-nucleotide markers identified in the Asian elephant—EMU03, EMU04, EMU06, EMU10, EMU11, EMU12, EMU13, EMU14, EMU15, and EMU17 [24]. Uniplex PCRs were performed for a 15 μL reaction volume, containing 1.5 μL 10× Taq buffer (TaKaRa Extaq Hot Start version, TaKaRa, Shiga, Japan), 1.5 μL of dNTP, 1.5 μL of 10 mg bovine serum albumin (BSA), 0.5 pM of both forward and reverse primer, 0.75U of Taq polymerase (TaKaRa Extaq Hot Start version, TaKaRa, Shiga, Japan), 5.75 μL of nuclease-free water, and 3 μL of template DNA. PCR started with an initial denaturation at 95 °C for 10 min, followed by 45 cycles of denaturation at 95 °C for 45 s, annealing at 58 °C for 45 s, and extension at 72 °C for 45 s, followed by a final extension at 72 °C for 10 min. PCRs were carried out in triplicate for each locus. All reactions included positive and negative controls to account for contamination and PCR failure. Reaction success was checked electrophoretically in 2% agarose gel. PCR amplification was carried out in three replicates and then subjected in triplicate to capillary electrophoresis in an ABI 3730 Automated Genetic Analyser along with Genescan LIZ500 internal size standard to identify alleles, which were then analyzed with GENEMAPPER 5.0 (Thermofisher Scientific, Waltham, USA). Consensus genotypes for a homozygote consistent in three replicates and a heterozygote in two replications were taken, and data generated at ten loci were used for further analysis. Mismatches in two loci were accepted and were manually re-examined to rule out scoring or entry errors. Recaptures were detected with the identity analysis module in CERVUS 3.0.7 [25]. The error rates in individual genotyping, ADO (allelic dropout), FA (false alleles), and successful PCRs were estimated with GIMLET v.1.3.3 [26]. GIMLET was also used to construct a consensus multi-locus genotype from a set of PCRs and to calculate genotyping error rates comparing the repeated genotypes and their consensus.

The genotyped data showed the occurrence of missing data across the originally 399 genotyped individuals and ten microsatellite loci. The percentage of missing data varied across loci (between 16 and 46%) and individuals (between 10 and 40%). Missing genotypes and genotyping errors cause bias in the genetic diversity estimates and also impact the accuracy of population structure inference [27]. For studies with low-quality DNA, the most-used approach is to eliminate problematic individuals or loci. Therefore, samples missing data in three microsatellite loci with over 30% of genotype calls were discarded, resulting in a final panel of seven loci. Of the 399 total individuals, 223 were observed with more than 15% missing genotypes at all loci. These individuals were hence excluded

from the analyses, resulting in a final panel of 176 individuals from the north (*n* = 136, NBR) and south (*n* = 40, ATR-KMTR) of the Palghat Gap. The Probability of Identity (P_{ID} and P_{IDsibs}) was calculated in CERVUS 3.0.7 and the Hardy–Weinberg Equilibrium (HWE) was estimated for each locus. We found homozygosity excess; therefore, we searched for evidence of null alleles using FreeNA [28] and sought to infer the most probable technical cause of departures from HWE. The frequency of null alleles was also calculated for each locus with FreeNA [28], using the maximum likelihood estimation from Dempster et al. [29].

We calculated pairwise, individual-by-individual (NxN) genetic distance for elephant genotypes after obtaining the proportion of shared alleles with Adegenet [30] in R version 3.5.3 [31]. A PCA-based genetic distance matrix was generated by calculating principal components from allele usage in the population [32].

2.3. Population Structure

Population differentiation was estimated by total and pairwise Fst [33], G_{st} [34], and Djost [35] values between the two regions (north and south of the Palghat Gap) using the R package in diveRsity [36] based on a confidence interval of 95% by bootstrap resampling (*n* = 9999). The partition of genetic variation within and among populations was estimated through Analysis of Molecular Variance (AMOVA) [37] with Arlequin 3.11 [38]. We tested for isolation by distance (IBD) using the Mantel test for correlations between pairwise genetic and geographic distances among individuals with GenALEx 6.5.

2.4. Slope Distribution Models

Landscape variables such as slope can be transformed by mathematical functions to obtain resistance rasters [17]. It is also informative to transform landscape variables based on movement data when available, as the transformation is likely to provide a better correlation between the genetic distance and the landscape distance [39]. To do so, we used 6688 location records of five radio-collared elephants ranging over parts of the NBR (Figure 1) in order to predict elephant distributions relative to slope. We did not observe any long-distance displacement, and our database is likely to represent daily foraging movement. We randomly extracted a maximum of one record per day per elephant and selected no more than 100 records per elephant (Appendix A) to minimize spatial autocorrelation and avoid the over-representation of some elephants. This reduced the database (SatDB) to 362 records.

All SatDB fixes were superimposed on the Shuttle Radar Topography Mission (SRTM) digital elevation model (DEM) with a spatial resolution of 3 arc seconds (approximately 90 m) [40]. Slope angles in degrees were extracted for each fix and transformed to their tangent (slope) in GRASS GIS [41]. The collars used to locate elephants were GPS+VHF Collars (African Wildlife Tracking Company) with a spatial accuracy of 5 to 10 m. We used a GPS (Trimble Juno SB with 2 to 5 m accuracy) to georeference the dung pile locations. Overall, the total error on the relative locations of the sampling points over the DEM was in the range of 30 m. As slopes are autocorrelated and as elephants in general use moderate slopes, the risk of introducing a bias towards steeper slopes was low. We did not notice outliers.

Model selection was carried out with the package fitdistrplus [42]. The best distribution followed a gamma model (see Results). The function [1-(gamma cdf)] ("cdf" for cumulative distribution function) represented decreasing elephant density.

Radio-collaring elephants in India is infrequent because of the conservation status of the species. As our sample size was small, we also utilized a slope distribution model obtained from 54 African savanna elephants (*Loxodonta africana*) in a hilly area [11] (Appendix B), evaluated from a 30 m spatial resolution DEM. A Kolmogorov–Smirnov test indicated that we could not reject the hypothesis that the distributions obtained with a 30 m or 90 m spatial resolution were similar (D = 0.139, *p* = 0.28). The model's cdf was adjusted to integrate to 1 to represent decreasing elephant density. The mass of the African

savanna elephant is close to that of the Asian elephant, and we expect slope usage to be similar under comparable conditions.

2.5. Resistance Maps

We produced a series of candidate resistance maps (Figure 2) with the R package raster [43], transforming the slope into resistance values varying between 1 and a maximum of 5, 10, 20, 40, and 80 [17]. We observed that elephants used slopes below 0.857 (40.6 degrees). Slopes equal to 0.857 were considered to offer maximum resistance and were given a prohibitive resistance of 100,000 together with canals and pipelines. The gamma transformations were carried out according to Equation (1):

$$R = 1 + (R_{max} - 1) \times F(slope), \tag{1}$$

where R is resistance, R_{max} is maximum resistance, and F is the cumulative distribution function of the empirical gamma distributions of elephant presence and slope varying between 0 and 0.857.

The power transformations followed Equation (2):

$$R = 1 + (R_{max} - 1) \times (slope/0.857)^p, \tag{2}$$

where p is the power of the transformation varying between $p = 0.1$, 0.5, 1.0, 2.0, and 4.0 [17], and other variables are defined as above in Equation (1). The power transformations change the shape of the function to explore non-linear relationships between landscape features and resistance to gene flow.

We also used the exponential model for the African savanna elephant [11] to produce resistance maps (Equation (3)):

$$R = 1 + (R_{max} - 1) \times ((87.36 - exp(-5.77 \times slope + 4.47))/87.36). \tag{3}$$

Varying R_{max} enables the optimization of the relative influence of variation in landscape features on resistance to gene flow [17,44]. Here, we did not compare multiple variables but a minimum resistance of 1 when $R_{max} = 5$ has a different effect on the least-cost path slope resistance than a minimum resistance of 1 with $R_{max} = 80$. The transformation scheme consequently helped explore this effect.

In total, 35 resistance maps (25 power transformations, 5 gamma transformations, and 5 exponential transformations) were produced. The least-cost path resistance matrix among the 176 genotyped elephants' locations was calculated with the R package sGD [45]. We included a Euclidean distance matrix as an alternative model to obtain 36 distance matrices.

2.6. Model Optimization and Gene Flow

The 36 distance matrices were correlated with the genetic distance matrix by applying linear mixed-effect models [46] with the R package "ResistanceGA" [47]. Candidate models were compared based on their AIC scores. The northern and southern elephant populations were considered independently and provided the same best model (Appendix C).

We used an individual-based approach to predict core areas and expected movement corridors on the best resistance model in the NBR. We considered as sources and destinations a set of 1194 simulated elephants in a regular grid within the NBR only. This grid represented a homogeneous distribution of adult elephants in the NBR at an overall density of ca. 0.45 km², the approximate elephant density of the NBR [20]. We used the UNICOR-resistant kernel [48] connectivity modeling option to detect core areas relative to slope, implemented with a 15,000 cost unit threshold. We applied the factorial least-cost path modeling method of UNICOR [49] to detect least-cost paths. The maximum cost unit threshold of 15,000 represented corridors outside the NBR that would not extend beyond areas where elephants had been observed in the recent past [21].

For both kernel and corridor maps, we assumed two opposite and extreme relationships between elephant movement and the boundary of the protected area. The first set of simulations considered the NBR boundary to be completely open. The second set of simulations made the NBR boundary impassable in order to represent the reserve as if it were self-contained.

3. Results

After excluding three microsatellite loci (EMU06, EMU13, and EMU15) and 223 individuals (55%) from the original dataset of 399 genotyped individuals, 176 elephants with more than 85% genotypes were used to estimate connectivity among elephant populations in the north and south of the Palghat Gap in the Western Ghats using occurrence and population genetics analyses. The P_{ID} and $P_{ID\,sib}$ values for seven loci were 1.7×10^{-7} and 2.1×10^{-3}, respectively, indicating that seven-loci genotypes were sufficient to identify unrelated individuals as well as siblings in the population. Null allele frequency across polymorphic loci was below 12% both north and south of the Palghat elephant populations. A low level of genotyping error was observed across the seven loci and most loci showed high amplification success, ranging between 89 and 97%. The mean allelic dropout (ADO) rate across loci was 0.06% and the false allele (FA) rate was 0.03%. All seven microsatellites were polymorphic with between four and 14 alleles per locus.

A moderate level of genetic differentiation (pairwise Fst = 0.08; Gst = 0.04, and Djost = 0.12) was observed between the two populations in the north and south of the Palghat Gap, suggesting limited genes. Pairwise values of Gst and Djost, which correct the dependency of Fst on the amount of within-population variation, were also moderate and statistically significant ($\alpha = 0.05$) based on 9999 bootstrap resamplings. Moreover, the global Fst and the Fst values for each locus were similar when calculated with and without estimating a null allele correction (Fst ENA = 0.077, Fst = 0.08). This shows that the presence of null alleles has not affected our calculations of genetic differentiation. AMOVA analyses revealed that 8% of the total variation was found among populations, while the rest (92%) was within populations ($p < 0.001$). The Mantel test of IBD was not significant (p values > 0.05) and yielded a very low correlation coefficient ($r_{XY} \leq 0.04$).

We evaluated seven candidate distribution models with the SatDB to describe the distributions of elephants relative to slope. The best distribution model was the gamma distribution (Table 1). The empirical SatDB distribution was close to its theoretical distribution (Kolmogorov–Smirnov statistic = 0.087). The estimated parameters of the gamma distributions were used to produce resistance layers. The gamma model and the exponential model (obtained for the African savanna elephant) were close to each other with the same average of 0.12 (6.8 deg) at this level of precision.

Table 1. Parameters of the gamma distribution obtained from the SatDB elephant locations.

Database	Shape (se.)	Rate (se.)	Average	Variance
SatDB	1.820 (0.125)	14.892 (1.175)	0.122	0.008

Gamma, power, the exponential transformations of slopes with varying R_{max}, and the Euclidean distance among elephants provided 36 landscape least-cost distance matrices (Table 2) among 176 elephants. The SatDB gamma-transformed slope had the lowest AIC at *Rmax* = 80 and was consequently the best model to explain gene flow in the studied landscape. It was valid over the entire WG, in the northern and the southern populations (Appendix C). The exponential distribution (*Rmax* = 80) was the next best model after two gamma-transformed models (with *Rmax* = 40 and 20) and the power model with *Rmax* = 80 and $p = 1.0$. The Euclidean distance had the second lowest support among the studied models.

Table 2. Correlation between least-cost path landscape distance with genetic distance measured by the AIC. The resistance raster models are indicated with the transformation, maximum resistance, and power applied to the slope.

| Transformation	*Rmax*	Power	AIC	Transformation	*Rmax*	Power	AIC
Gamma	80	-	43,499	Exponential	5	-	43,661
Gamma	40	-	43,513	Power	10	0.5	43,664
Gamma	20	-	43,530	Power	20	2.0	43,679
Power	80	1.0	43,538	Power	5	0.5	43,701
Exponential	80	-	43,546	Power	5	1.0	43,706
Exponential	40	-	43,552	Power	10	2.0	43,710
Power	40	1.0	43,567	Power	80	4.0	43,715
Exponential	20	-	43,569	Power	80	0.1	43,730
Gamma	10	-	43,572	Power	40	4.0	43,730
Power	80	2.0	43,606	Power	40	0.1	43,731
Exponential	10	-	43,607	Power	20	0.1	43,732
Power	20	1.0	43,613	Power	10	0.1	43,735
Power	80	0.5	43,614	Power	5	2.0	43,736
Power	40	0.5	43,626	Power	5	0.1	43,740
Gamma	5	-	43,635	Power	20	4.0	43,741
Power	20	0.5	43,643	Power	10	4.0	43,754
Power	40	2.0	43,646	Euclidean	-	-	43,761
Power	10	1.0	43,661	Power	5	4.0	43,766

Using the best resistance model, we estimated that in approximately 28% of the NBR, the probability of the presence of elephants was below 0.05. The topographically inaccessible areas occur mostly in the southern and northeastern parts of the reserve. Most reserves in the Western Ghats seem to be in sub-optimal habitats as far as slope is concerned (Figure 3).

Core areas relative to slope were often found outside of the PA boundaries (Figure 4a). When the boundary was made impassable, the core areas were split (Figure 4b (i, iii)), populations isolated (Figure 4b (ii, iv)), and connectivity disrupted around the NBR (Figure 4b (v)). Corridors tended to occur outside the NBR whenever the reserve boundary had a U shape (Figure 5a,c), except when a river formed the boundary (Figure 5a, southern part). When the boundary was made impassable, corridors still existed, and connectivity was preserved wherever the terrain was flat (Figure 5b). However, enclosing the reserve removed corridors that circled mountain outcrops, and some corridors within the NBR also disappeared (compare Figure 5c,d).
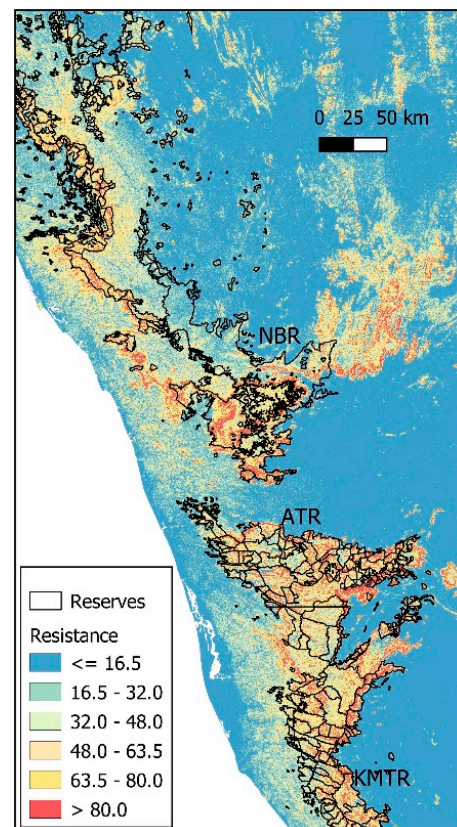
Figure 3. Representation of elephant gene flow resistance over the Western Ghats of India relative to slope (see text for detail). Gene flow resistance would be very high beyond the reserve limits if other factors such as land use had been taken into consideration. Reserve boundaries were obtained from the India Biodiversity Portal (https://indiabiodiversity.org/ accessed on 23 March 2020).
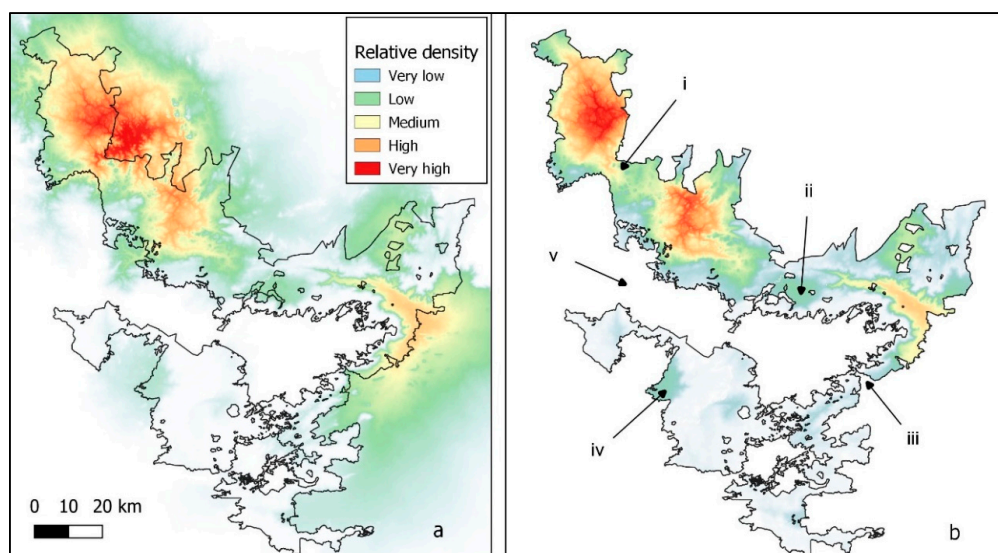
Figure 4. Elephant population core areas relative to slope with boundary completely open to elephant movement (**a**). Elephant population core areas relative to slope with boundary completely closed to elephant movement (**b**) with (i) and (iii) split core areas, (ii) and (iv) isolated populations, and (v) the severance of a major connection outside the NBR. Reserve boundaries were obtained from the India Biodiversity Portal (https://indiabiodiversity.org/ accessed on 23 March 2020).
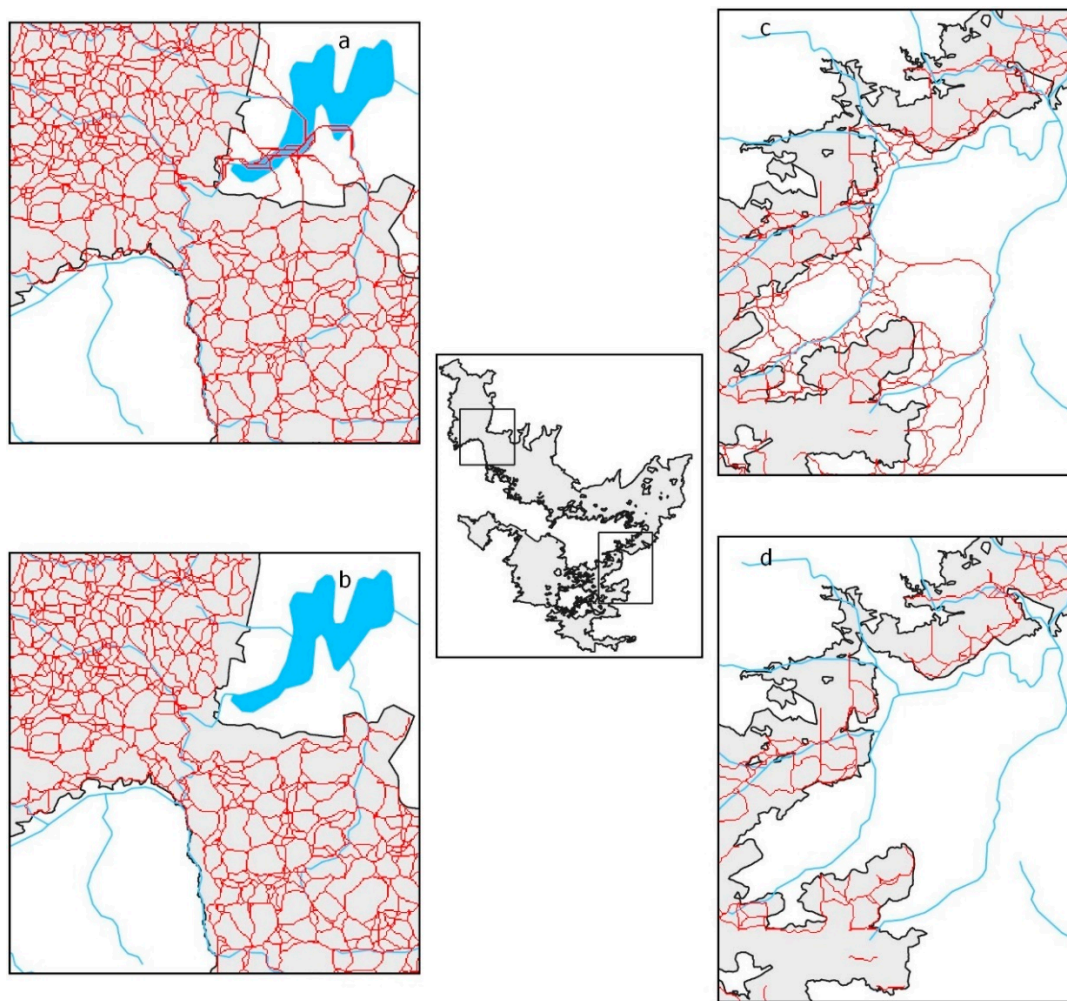
Figure 5. Elephant corridors in the Nilgiri Biosphere Reserve with boundaries open to movement (**a**,**c**) and with boundaries closed to movement (**b**,**d**). Water bodies (in blue), including an artificial lake, were not considered to oppose resistance to movement.

4. Discussion

Protected areas are increasingly isolated due to land-use changes in the surrounding matrix [50,51], with negative outcomes for the genetic makeup of species [52]. Isolation also increases the edge effect [53], plant invasion [54], and exposure to degradation [55]. Moreover, the transition between ecosystems and human-dominated areas is often abrupt due to activities and people who are intolerant of wandering wildlife. To avoid problems, managers often choose to enclose PAs [56], which can further affect population connectivity, as suggested by the present study.

Genetic distance among individuals can be used to measure gene flow over the landscape and help test whether fencing PAs can by itself fragment populations of particular species. We chose to collect noninvasive elephant DNA samples, but genetic material from scats may generate missing genotypes and errors associated with the amplification of minute quantities of DNA, which may impact downstream analyses [27,57]. Despite stringent control measures for allele scoring, our replicate genotypes revealed missing and null alleles.

Three independent series of PCRs helped decrease the probability of genotyping errors in the consensus individual genotypes. To obtain reliable estimates of genetic variation and population subdivision (pairwise Fst), we kept the missing data below a frequency of 0.3 and thus excluded three loci and a substantial number of individuals (~55%) from the final data set, as in Parida et al. [23].

The two populations north and south of the Palghat Gap in the Western Ghats showed moderate genetic differentiation (Fst (0.08), Gst (0.04), and Djost (0.12)), suggesting that some restriction in gene flow occurred between these populations. These results agree with De et al. [22], who found similar values (Fst = 0.07 and Djost = 0.10) along the Western Ghats using 14 microsatellites. However, these values are smaller when compared to those observed in elephant populations across India (e.g., [22,58]).

In order to compare genetic distance and landscape distance, resistance rasters had to be created as competing hypotheses. These resistance maps were slope transformation rasters over most of the WG. In particular, it was important to establish a slope occupancy model for the Asian elephant, as statistical models derived from empirical movement data may correlate better with genetic distance than power transformations [39]. The occupancy model was obtained from the location records of five elephants ranging over parts of the NBR. The database was considerably reduced for statistical reliability by avoiding autocorrelation and the over-representation of some elephants. The best slope occupancy distribution model was a gamma probability density function (Table 1). Since the model was obtained with a small sample size, we compared it to that obtained from the African savanna elephant [11]. The distribution models were close to each other; the exponential model from Wall et al. [11] had the same average slope (or tangent) of 0.12 (or 6.8 degrees) as the gamma model at this level of precision.

In total, 36 resistance rasters were produced from (i) a slope occupancy model for the Asian elephant, (ii) the power transformation of slopes, and (iii) a slope occupancy model for the African savanna elephant. The genetic distance matrix among 176 individuals was correlated to the 36 landscape distance matrices obtained from the resistance rasters. The highest correlation (lowest AIC) between genetic distance and landscape distance was obtained with the terrain slope transformed with the empirical gamma distribution with resistance varying between 1 and 80 (Table 2). This model performed better than the exponential distribution or any other power transformation. Among the transformation models evaluated, it best represented resistance to gene flow at the landscape level (Figure 3). This confirms that the occupancy model for the elephant is robust despite the small sample size from which it was derived. It is to be noted that the slope alone, again expressed in tangent, with no power transformation (power = 1.0) and with Rmax = 80 (Table 2), provides a simple but satisfactory resistance model.

Gene flow among populations is usually measured by pairwise F_{ST} values. Instead, we used here individual-based genetic distances for all alleles in the population. This genetic distance matrix was then correlated with landscape distance matrices. The best correlation between genetic and landscape distances provided the resistance map that was also the best possible depiction of resistance to gene flow over the landscape (Figure 3). Since the correlation was much better than for Euclidean distance, it can be concluded that gene flow is partially controlled by terrain slope, as expected from the energetics of movement for heavier animals [59].

From Figure 3, it seems that most reserves in the WG were established on rough terrain probably less suitable for agriculture. Therefore, gene flow is constrained over most of the remaining elephant range. The NBR contains near-optimal habitats in the northern reserves (Nagar Hole, Bandipur, and Mudumalai Tiger Reserves), and field surveys provide the highest elephant density in these areas [20]. According to the best resistance model, approximately 28% of the NBR's extent (5670 km^2) has terrain with a probability of elephant presence below 5%. These topographically inaccessible areas occur mostly in the southern and northeastern parts of the reserve. Elephant censuses rely on the block count method [60] with extrapolation from surveyed blocks to other blocks. As census data do not seem to be available to the public, it is impossible to verify the impact of terrain on density estimates. There is a risk of overestimating the elephant population by a failure to adjust for topographical accessibility and censuses conducted to date should be evaluated for potential bias leading to overestimating population density.

To assess NBR elephant core areas and movement corridors in relation to topographical slope, we used UNICOR [49]. We adopted simplified assumptions considering that (i) slope was the only variable affecting elephant movements; (ii) the matrix outside the protected area network was similar to the elephant habitat, except that elephants were originating only from within the NBR; and (iii) to simulate the closure of the NBR, the matrix was completely closed to elephant movement. These assumptions are obvious simplifications: the terrain slope is one among many variables interfering with elephant movement; the matrix outside elephant habitats differs from the habitat within, and enclosures rarely seal entire reserves.

With these models, we observed that a considerable amount of connectivity exists outside the NBR (Figure 4a). In particular, two major core areas, one in the northwest and the other in the east of the NBR, extend beyond the reserve: this land is relatively flat and is a natural range for dispersal. Of course, the core areas beyond the NBR boundary are now utilized for agriculture but would otherwise attract elephants due to their relatively flat terrain. The Palghat Gap, the major interruption of the WG, is relatively flat and consequently easily negotiable by elephants. Even though it could be considered a major barrier for animals with little vagility or even for elephants [61], it seems to be an obstacle to elephants only because of land transformation to agriculture and settlements. This hypothesis is in agreement with the likelihood of recent historical connectivity [22]. In the south of the NBR particularly, the reserve boundary tends to follow contour lines that mark the difference between steep and flat land (following the maxima of the second derivative of elevation) suitable for agriculture (Figure 1). Therefore, whenever the reserve boundary is digitated, i.e., forms finger-like protrusions into the matrix, the land within the protrusions that lie outside the reserve has high connectivity and contains least-cost passages (Figure 5a,c). Remarkably, boundaries that are established along rivers (southwestern part of Figure 5a) do not have external corridors because the least-cost paths follow rivers.

When the reserve is totally barricaded (Figure 4b), connectivity reduces (Figure 4b (i)) or breaks off (Figure 4b (iii,v)). Core areas become more compact and isolated (Figure 4b (i,ii,iv)). Corridors still exist on flat terrain within the reserve (Figure 5b) but can be interrupted by hilly habitats within the reserve (Figure 4d).

The proximate causes of animal dispersal are many, including food availability, search strategies, or patch isolation [62]. Elephants are wide-ranging animals, possibly in response to habitat productivity [63], among other things. It has been proposed that the search for food is a major reason for elephants venturing out of their protected areas [64]. We show in this study that this might be more nuanced. Elephants are highly mobile and the difficulties in negotiating steep terrain might bring them near villages that occupy valleys. This by itself might be a cause of incidents with humans.

5. Conclusions

Over millennia, elephants ranged from India and Southeast Asia to China, but due to anthropic pressures, they have been progressively restricted to mountain chains where they now exist as remnant populations [65]. We show that terrain slope partly controls gene flow for the Asian elephant. The sensitivity of this animal to slope raises the question of whether mountainous habitats, where most elephant reserves are found today, are best-suited as PAs. On islands, elephants tend to get smaller as an adaptation to the restricted area [66], but the effect of steep terrain on the elephant's evolution is unknown. With this uncertainty, reserves on relatively flat terrain should be strictly preserved, as they may be more suitable for this animal.

The study also suggests that some incidents with humans may have their origin in the design of reserves relative to slope. Villages often occupy valleys and lie in areas that are easier for elephants to negotiate. Villages in narrow valleys probably need specially designed protection measures that would also maintain elephant population connectivity.

Lastly, we demonstrated that closing reserves without taking into consideration the boundary position relative to slopes can have negative impacts on gene flow within reserves.

With the increasing human domination of landscapes, managers often prefer enclosing elephant reserves to any other wildlife-friendly solution such as maintaining corridors [67], buffering with appropriate crops [68], or more generally adopting biodiversity-based land management [69]. The minimum requirement before fencing, however, is to verify that elephants have sufficient buffer space between the slope of a mountain and the fences in order to maintain the possibility of moving from one valley to another.

Appendix A

In order to predict elephant distributions relative to slope we used 6688 location records of elephants ranging over parts of the Nilgiri Biosphere Reserve (Figure 1). The locations were obtained from the satellite telemetry of four bulls and one cow over a period of nine years (2010–2019). The number of radio-collared elephants in India is low because there is a reluctance to undertake a procedure that can be dangerous for an endangered species. The temporal sampling interval varied among elephants from one record every two days to approximately one record per hour (Table A1). Slope records were strongly spatially autocorrelated (Moran I = 0.3952, expected = -0.0003, sd = 0.0019, $p << 0.001$), and the number of records per elephant varied between 86 and 2695. In order to reduce spatial autocorrelation and avoid the over-representation of some elephants, we randomly (i) extracted a maximum of one record per day per elephant, and (ii) selected no more than 100 records per elephant. This reduced the database (SatDB) to 362 records.

Table A1. Comparison of resistance model correlation with genetic distance.

Elephant	Start Date	End Date	Number of Records	Number of Days	Records per Day	Same Locations
Sat4	03/01/13	08/22/16	1752	1270	1.4	9
Sat2	05/23/13	12/14/13	2695	205	13.1	14
69c5	06/07/10	11/22/10	105	168	0.6	2
59b6	10/24/10	11/16/10	86	23	3.7	4
mdm	12/19/18	04/04/19	2089	106	19.7	10

Appendix B

A total of 54 African savanna elephants were radio-collared [11]. The number of "fixes" relative to the terrain slope were grouped in one-degree bins. From the scatter plot ([11] supplement) we extracted the gradient and elephant fix density with WebPlotDigitizer (https://automeris.io/WebPlotDigitizer/ accessed on 15 February 2020). The center value of each bin was 0.5, 1.5, . . . , 29.5 degrees, which allowed the examination of the error made in extracting values. The maximum deviation was 0.0385 (less than 5% of a degree) and the standard deviation of error was 3.22×10^{-4} degrees. We considered that the error obtained by extracting data from the figure was negligible. We fitted a linear model over the gradient and log-transformed density. One data point with zero density appeared to be an outlier and was eliminated. The linear model was highly significant ($R^2 = 0.81$, n = 29, $p <<< 0.001$) with parameters: log(density) = −5.774.gradient + 4.47.

Appendix C

Table A2. Correlation between least-cost path landscape distance with genetic distance measured by the AIC. The resistance raster models are indicated with the transformation, maximum resistance, and power applied to the slope.

Northern Population				**Southern Population**			
Transformation	*Rmax*	**Power**	**AIC**	**Transformation**	*Rmax*	**Power**	**AIC**
Gamma	80	-	26,569	Gamma	80	-	2714
Gamma	40	-	26,592	Gamma	40	-	2731
Power	80	1.0	26,618	Gamma	20	-	2749
Gamma	20	2.0	26,622	Exponential	80	-	2752
Power	40	1.0	26,640	Power	80	1.0	2756
Power	80	2.0	26,643	Exponential	40	-	2758
Exponential	80	-	26,645	Gamma	10	-	2764
Exponential	40	-	26,653	Power	40	1.0	2765
Gamma	10	-	26,654	Exponential	20	-	2766
Exponential	20	-	26,665	Power	80	2.0	2768
Power	20	1.0	26,669	Exponential	10	1.0	2774
Power	40	2.0	26,684	Power	20	1.0	2775
Exponential	10	-	26,684	Power	80	0.5	2777
Gamma	5	-	26,695	Gamma	5	0.5	2777
Power	80	0.5	26,695	Power	40	0.5	2778
Power	40	0.5	26,699	Power	40	2.0	2780
Power	10	1.0	26,706	Power	20	0.5	2781
Power	20	0.5	26,706	Exponential	5	-	2783
Power	20	2.0	26,714	Power	10	1.0	2784
Exponential	5	-	26,715	Power	10	0.5	2785
Power	10	0.5	26,717	Power	20	2.0	2787
Power	5	0.5	26,736	Power	5	1.0	2790
Power	5	1.0	26,738	Power	5	0.5	2790
Power	10	2.0	26,741	Power	10	2.0	2791
Power	80	4.0	26,745	Power	80	4.0	2791
Power	80	0.1	26,751	Power	5	2.0	2793
Power	40	0.1	26,751	Power	40	4.0	2793
Power	20	0.1	26,752	Power	20	4.0	2795
Power	10	0.1	26,754	Power	10	4.0	2796
Power	40	4.0	26,757	Power	5	4.0	2797
Power	5	0.1	26,758	Euclidean	-	-	2798
Power	5	2.0	26,760	Power	5	0.1	2801
Power	20	4.0	26,765	Power	10	0.1	2803
Power	10	4.0	26,774	Power	20	0.1	2803
Euclidean	-	-	26,781	Power	40	0.1	2804
Power	5	4.0	26,782	Power	80	0.1	2804

References

1. West, P.; Igoe, J.; Brockington, D. Parks and peoples: The social impact of protected areas. *Annu. Rev. Anthropol.* **2006**, *35*, 251–277. [CrossRef]
2. Wittemyer, G.; Elsen, P.; Bean, W.T.; Burton, A.C.O.; Brashares, J.S. Accelerated human population growth at protected area edges. *Science* **2008**, *321*, 123–126. [CrossRef] [PubMed]
3. Jones, K.R.; Venter, O.; Fuller, R.A.; Allan, J.R.; Maxwell, S.L.; Negret, P.J.; Watson, J.E.M. One-third of global protected land is under intense human pressure. *Science* **2018**, *360*, 788–791. [CrossRef] [PubMed]
4. Watson, J.E.M.; Shanahan, D.F.; Di Marco, M.; Allan, J.; Laurance, W.F.; Sanderson, E.W.; Mackey, B.; Venter, O. Catastrophic declines in wilderness areas undermine global environment targets. *Curr. Biol.* **2016**, *26*, 2929–2934. [CrossRef]
5. Shaffer, L.J.; Khadka, K.K.; Van Den Hoek, J.; Naithani, K.J. Human-elephant conflict: A review of current management strategies and future directions. *Front. Ecol. Evol.* **2019**, *6*, 235. [CrossRef]
6. Fernando, P.; Ekanayaka, S.K.K.; Pastorini, J. The elephant at the fence: Almsman, panhandler, friend or foe? *Eur. J. Wildl. Res.* **2020**, *66*, 97. [CrossRef]
7. Kalam, T.; Puttaveeraswamy, T.A.; Srivastava, R.K.; Puyravaud, J.-P.; Davidar, P. Spatial aggregation and specificity of incidents with wildlife make tea plantations in southern India potential buffers with protected areas. *J. Threat. Taxa* **2020**, *12*, 16478–16493. [CrossRef]
8. Wilkinson, C.E.; McInturff, A.; Kelly, M.; Brashares, J.S. Quantifying wildlife responses to conservation fencing in East Africa. *Biol. Conserv.* **2021**, *256*, 109071. [CrossRef]
9. Olivier, R. Distribution and status of the Asian elephant. *Oryx* **1978**, *14*, 379–424. [CrossRef]
10. Feng, L.; Zhang, L. Habitat selection by Asian elephant (*Elephas maximus*) in Xishuangbanna, Yunnan, China. *Acta Theriol. Sin.* **2005**, *25*, 229–236.
11. Wall, J.; Douglas-Hamilton, I.; Vollrath, F. Elephants avoid costly mountaineering. *Curr. Biol.* **2006**, *16*, R527–R529. [CrossRef]
12. Speakman, J.R.; Król, E. Maximal heat dissipation capacity and hyperthermia risk: Neglected key factors in the ecology of endotherms. *J. Anim. Ecol.* **2010**, *79*, 726–746. [CrossRef] [PubMed]
13. Schmidt-Nielsen, K. *Scaling: Why Is Animal Size So Important?* Cambridge University Press: Cambridge, UK; New York, NY, USA, 1984; ISBN 978-0-521-26657-4.
14. Wheatley, R.; Buettel, J.C.; Brook, B.W.; Johnson, C.N.; Wilson, R.P. Accidents alter animal fitness landscapes. *Ecol. Lett.* **2021**, *24*, 920–934. [CrossRef] [PubMed]
15. Balkenhol, N.; Cushman, S.A.; Storfer, A.T.; Waits, L.P. (Eds.) *Landscape Genetics*; John Wiley & Sons, Ltd.: Chichester, UK, 2015; ISBN 978-1-118-52525-8.
16. Peterson, E.E.; Hanks, E.M.; Hooten, M.B.; Ver Hoef, J.M.; Fortin, M.-J. Spatially structured statistical network models for landscape genetics. *Ecol. Monogr.* **2019**, *89*, e01355. [CrossRef]
17. Shirk, A.J.; Wallin, D.O.; Cushman, S.A.; Rice, C.G.; Warheit, K.I. Inferring landscape effects on gene flow: A new model selection framework. *Mol. Ecol.* **2010**, *19*, 3603–3619. [CrossRef]
18. Ruiz-González, A.; Gurrutxaga, M.; Cushman, S.A.; Madeira, M.J.; Randi, E.; Gómez-Moliner, B.J. Landscape genetics for the empirical assessment of resistance surfaces: The European pine marten (*Martes martes*) as a target-species of a regional ecological network. *PLoS ONE* **2014**, *9*, e110552. [CrossRef]
19. Myers, N.; Mittermeier, R.; Mittermeier, C.; da Fonseca, G.; Kent, J. Biodiversity hotspots for conservation priorities. *Nature* **2000**, *403*, 853–858. [CrossRef]
20. Baskaran, N. An overview of Asian elephants in the Western Ghats, southern India: Implications for the conservation of Western Ghats ecology. *J. Threat. Taxa* **2013**, *5*, 4854–4870. [CrossRef]
21. Gubbi, S.; Swaminath, M.H.; Poornesha, H.C.; Bhat, R.; Raghunath, R. An elephantine challenge: Human–elephant conflict distribution in the largest Asian elephant population, southern India. *Biodivers. Conserv.* **2014**, *23*, 633–647. [CrossRef]
22. De, R.; Sharma, R.; Davidar, P.; Arumugam, N.; Sedhupathy, A.; Puyravaud, J.-P.; Selvan, K.M.; Rahim, P.P.A.; Udayraj, S.; Parida, J.; et al. Pan-India population genetics signifies the importance of habitat connectivity for wild Asian elephant conservation. *Glob. Ecol. Conserv.* **2021**, *32*, e01888. [CrossRef]
23. Parida, J.; Sharma, R.; De, R.; Kalam, T.; Sedhupathy, A.; Digal, D.K.; Reddy, P.A.; Goyal, S.P.; Puyravaud, J.-P.; Davidar, P. Genetic characterisation of fragmented Asian elephant populations with one recent extinction in its eastern-central Indian range. *Ecol. Genet. Genom.* **2022**, *24*, 100132. [CrossRef]
24. Kongrit, C.; Siripunkaw, C.; Brockelman, W.Y.; Akkarapatumwong, V.; Wright, T.F.; Eggert, L.S. Isolation and Characterization of Dinucleotide Microsatellite Loci in the Asian Elephant (*Elephas Maximus*). *Mol. Ecol. Resour.* **2008**, *8*, 175–177. [CrossRef] [PubMed]
25. Kalinowski, S.T.; Taper, M.L.; Marshall, T.C. Revising how the computer program Cervus accommodates genotyping error increases success in paternity assignment: Cervus likelihood model. *Mol. Ecol.* **2007**, *16*, 1099–1106. [CrossRef] [PubMed]
26. Valière, N. Gimlet: A computer program for analysing genetic individual identification data: Program note. *Mol. Ecol. Notes* **2002**, *2*, 377–379. [CrossRef]
27. Pompanon, F.; Bonin, A.; Bellemain, E.; Taberlet, P. Genotyping errors: Causes, consequences and solutions. *Nat. Rev. Genet.* **2005**, *6*, 847–859. [CrossRef]

28. Chapuis, M.-P.; Estoup, A. Microsatellite null alleles and estimation of population differentiation. *Mol. Biol. Evol.* **2007**, *24*, 621–631. [CrossRef]

29. Dempster, A.P.; Laird, N.M.; Rubin, D.B. Maximum likelihood from incomplete data via the *EM* algorithm. *J. R. Stat. Soc. Ser. B Methodol.* **1977**, *39*, 1–22. [CrossRef]

30. Jombart, T. Adegenet: A R package for the multivariate analysis of genetic markers. *Bioinformatics* **2008**, *24*, 1403–1405. [CrossRef]

31. R Core Team. *R: A Language and Environment for Statistical Computing*, R version 4.0.0 (24-04-2020); R Core Team: Vienna, Austria, 2020.

32. Shirk, A.J.; Landguth, E.L.; Cushman, S.A. A comparison of individual-based genetic distance metrics for landscape genetics. *Mol. Ecol. Resour.* **2017**, *17*, 1308–1317. [CrossRef]

33. Weir, B.S.; Cockerham, C.C. Estimating *F*-statistics for the analysis of population structure. *Evolution* **1984**, *38*, 1358–1370. [CrossRef]

34. Nei, M. Genetic distances between populations. *Am. Nat.* **1972**, *106*, 283–292. [CrossRef]

35. Jost, L. G_{ST} and its relatives do not measure differentiation. *Mol. Ecol.* **2008**, *17*, 4015–4026. [CrossRef] [PubMed]

36. Keenan, K.; McGinnity, P.; Cross, T.F.; Crozier, W.W.; Prodöhl, P.A. DiveRsity: An R package for the estimation and exploration of population genetics parameters and their associated errors. *Methods Ecol. Evol.* **2013**, *4*, 782–788. [CrossRef]

37. Excoffier, L.; Smouse, P.E.; Quattro, J.M. Analysis of molecular variance inferred from metric distances among DNA haplotypes: Application to human mitochondrial DNA restriction data. *Genetics* **1992**, *131*, 479–491. [CrossRef]

38. Excoffier, L.; Laval, G.; Schneider, S. Arlequin (Version 3.0): An integrated software package for population genetics data analysis. *Evol. Bioinform. Online* **2005**, *1*, 47–50. [CrossRef]

39. Cushman, S.A.; Lewis, J.S. Movement behavior explains genetic differentiation in American black bears. *Landsc. Ecol.* **2010**, *25*, 1613–1625. [CrossRef]

40. Reuter, H.I.; Nelson, A.; Jarvis, A. An evaluation of void filling interpolation methods for SRTM data. *Int. J. Geogr. Inf. Sci.* **2007**, *21*, 983–1008. [CrossRef]

41. GRASS Development Team. *Geographic Resources Analysis Support System (GRASS) Software*; Version 7.8.2; Open Source Geospatial Foundation: Beaverton, OR, USA, 2020.

42. Delignette-Muller, M.-L.; Dutang, C. Fitdistrplus: An R package for fitting distributions. *J. Stat. Softw.* **2015**, *64*, 1–34. [CrossRef]

43. Hijmans, R.J. *Raster: Geographic Data Analysis and Modeling*, R package version 3.3-13; CRAN: Vienna, Austria, 2020.

44. Castillo, J.A.; Epps, C.W.; Davis, A.R.; Cushman, S.A. Landscape effects on gene flow for a climate-sensitive montane species, the American Pika. *Mol. Ecol.* **2014**, *23*, 843–856. [CrossRef]

45. Shirk, A.J.; Landguth, E.L.; Cushman, S.A. A comparison of regression methods for model selection in individual-based landscape genetic analysis. *Mol. Ecol. Resour.* **2018**, *18*, 55–67. [CrossRef]

46. Shirk, A.J.; Cushman, S.A. sGD: Software for estimating spatially explicit indices of genetic diversity. *Mol. Ecol. Resour.* **2011**, *11*, 922–934. [CrossRef] [PubMed]

47. Peterman, W.E. ResistanceGA: An R package for the optimization of resistance surfaces using genetic algorithms. *Methods Ecol. Evol.* **2018**, *9*, 1638–1647. [CrossRef]

48. Compton, B.W.; McGarigal, K.; Cushman, S.A.; Gamble, L.R. A resistant-kernel model of connectivity for amphibians that breed in vernal pools. *Conserv. Biol.* **2007**, *21*, 788–799. [CrossRef] [PubMed]

49. Landguth, E.L.; Hand, B.K.; Glassy, J.; Cushman, S.A.; Sawaya, M.A. UNICOR: A species connectivity and corridor network simulator. *Ecography* **2012**, *35*, 9–14. [CrossRef]

50. DeFries, R.; Hansen, A.; Newton, A.C.; Hansen, M.C. Increasing isolation of protected areas in tropical forests over the past twenty years. *Ecol. Appl.* **2005**, *15*, 19–26. [CrossRef]

51. Saura, S.; Bertzky, B.; Bastin, L.; Battistella, L.; Mandrici, A.; Dubois, G. Global trends in protected area connectivity from 2010 to 2018. *Biol. Conserv.* **2019**, *238*, 108183. [CrossRef]

52. Frankham, R.; Ballou, J.D.; Briscoe, D.A. *Introduction to Conservation Genetics*, 2nd ed.; Cambridge University Press: Cambridge, UK; New York, NY, USA, 2010; ISBN 978-0-521-87847-0.

53. Woodroffe, R.; Ginsberg, J.R. Edge Effects and the extinction of populations inside protected areas. *Science* **1998**, *280*, 2126–2128. [CrossRef]

54. Pauchard, A.; Alaback, P.B. Influence of elevation, land use, and landscape context on patterns of alien plant invasions along roadsides in protected areas of South-Central Chile. *Conserv. Biol.* **2004**, *18*, 238–248. [CrossRef]

55. Burivalova, Z.; Butler, R.A.; Wilcove, D.S. Analyzing Google Search data to debunk myths about the public's interest in conservation. *Front. Ecol. Environ.* **2018**, *16*, 509–514. [CrossRef]

56. Cushman, S.A.; Elliot, N.B.; Macdonald, D.W.; Loveridge, A.J. A multi-scale assessment of population connectivity in African lions (*Panthera leo*) in response to landscape change. *Landsc. Ecol.* **2016**, *31*, 1337–1353. [CrossRef]

57. Broquet, T.; Petit, E. Quantifying genotyping errors in noninvasive population genetics. *Mol. Ecol.* **2004**, *13*, 3601–3608. [CrossRef] [PubMed]

58. Vidya, T.N.C.; Fernando, P.; Melnick, D.J.; Sukumar, R. Population genetic structure and conservation of Asian elephants (*Elephas maximus*) across India. *Anim. Conserv.* **2005**, *8*, 377–388. [CrossRef]

59. Halsey, L.G.; White, C.R. A different angle: Comparative analyses of whole-animal transport costs when running uphill. *J. Exp. Biol.* **2017**, *220*, 161–166. [CrossRef] [PubMed]

60. Baskaran, N.; Sukumar, R. *Karnataka Elephant Census 2010*; Centre for Ecological Sciences, Indian Institute of Science & Asian Nature Conservation Foundation; Indian Institute of Science: Bangalore, India, 2011; p. 33.

61. Vidya, T.N.C.; Sukumar, R. Social organization of the Asian elephant (*Elephas maximus*) in southern India inferred from microsatellite DNA. *J. Ethol.* **2005**, *23*, 205–210. [CrossRef]

62. Bowler, D.E.; Benton, T.G. Causes and consequences of animal dispersal strategies: Relating individual behaviour to spatial dynamics. *Biol. Rev.* **2005**, *80*, 205–225. [CrossRef]

63. Fernando, P.; Wikramanayake, E.D.; Janaka, H.K.; Jayasinghe, L.K.A.; Gunawardena, M.; Kotagama, S.W.; Weerakoon, D.; Pastorini, J. Ranging behavior of the Asian elephant in Sri Lanka. *Mamm. Biol.* **2008**, *73*, 2–13. [CrossRef]

64. Sukumar, R. Ecology of the Asian elephant in southern India. II. Feeding habits and crop raiding patterns. *J. Trop. Ecol.* **1990**, *6*, 33–53. [CrossRef]

65. Trautmann, T.R. *Elephants and Kings: An Environmental History*; The University of Chicago Press: Chicago, IL, USA, 2015; ISBN 978-0-226-26422-6.

66. Baleka, S.; Herridge, V.L.; Catalano, G.; Lister, A.M.; Dickinson, M.R.; Di Patti, C.; Barlow, A.; Penkman, K.E.H.; Hofreiter, M.; Paijmans, J.L.A. Estimating the dwarfing rate of an extinct Sicilian elephant. *Curr. Biol.* **2021**, *31*, 3606–3612.E7. [CrossRef]

67. Davidar, E.R.C.; Davidar, P.; Davidar, P.; Puyravaud, J.-P. Elephant (*Elephas maximus* Linnaeus Proboscidea: Elephantidae) migration paths in the Nilgiri Hills, India in the late 1970s. *J. Threat. Taxa* **2012**, *4*, 3284–3293. [CrossRef]

68. Santiapillai, C.; Wijeyamohan, S.; Bandara, G.; Athurupana, R.; Dissanayake, N.; Read, B. An assessment of the human-elephant conflict in Sri Lanka. *Ceylon J. Sci. Biol. Sci.* **2010**, *39*, 21–33. [CrossRef]

69. Kremen, C.; Merenlender, A.M. Landscapes that work for biodiversity and people. *Science* **2018**, *362*, eaau6020. [CrossRef] [PubMed]